Proceedings of the Combustion Institute 40 (2024) 105575

Contents lists available at ScienceDirect

Proceedings of the Combustion Institute

journal homepage: www.elsevier.com/locate/proci

A novel model for solid fuel combustion with particle migration

Jingyuan Zhang [a], Corinna Schulze-Netzer [a,*], Tian Li [a,b], Terese Løvås [a]

[a] *Department of Energy and Process Engineering, NTNU Norwegian University of Science and Technology, Kolbjørn Hejes vei 1b, 7491 Trondheim, Norway*
[b] *RISE Fire Research, Tillerbruvegen 202, 7092 Tiller, Norway*

ARTICLE INFO

Keywords:
Solid fuel
Porous medium
Fixed-bed
CFD
Bed collapsing

ABSTRACT

Solid fuel conversion in a fixed-bed is a challenging modelling task due to different time and length scales and the importance of heat transfer mechanisms. The current study aims to propose a novel model that can capture all the main features of the conversion of fuel bed while maintaining a moderate computational cost. The model is based on the commonly applied porous media approach, which describes the solid phase using an Eulerian framework. A layered particle submodel with four types of solids, wet wood, dry wood, char, and ash, is implemented to account for different conversion stages. At each computational cell, a matrix is used to record the information on all the properties of the four types of solids, including the number and volume of particles. The model allows the exchange of particles between cells, thus capable of simulating the motion of the fuel bed during conversion, such as bed collapsing. In addition, the new model can efficiently calculate heat transfer between particles and particles and fluid in each computational cell. The proposed model is validated against a series of experiments on biomass conversion in a rectangular fixed-bed combustor operated in a counter-current mode with various air supply rates. Good agreement with experiments was found even at the limited combustion regime. With the overall low computational cost generated by the bed model, the proposed model framework has the potential to efficiently simulate a wide range of solid fuel conversion processes at a large scale, not only in fixed-beds but also in moving beds and rotary kilns.

1. Introduction

As the substitute energy source for fossil fuel, biomass and municipal solid waste (MSW) have gained increasing interest. Fixed-bed, also termed packed bed, is one of the most widely used furnaces in biomass/MSW-to-energy plants thanks to its flexibility of accommodating fuels with strongly varying properties, such as size and moisture content, at low construction and operating costs [1]. In biomass/MSW-to-energy plants, the combustion process contributes to the major part of exergy and efficiency losses [2] and, hence, is constantly the target for further optimization. Computational fluid dynamics simulations (CFD) are commonly used to study and optimize the multi phase nature of such systems. For these optimizations, improved CFD models of the fuel conversion in the bed are however needed to allow for design process with sufficient detail and predictive character at an affordable computational cost.

Eulerian models, e.g., the porous media model (PMM), can simulate the thermal conversion of the fuel bed in a large-scale furnace with efficient computational cost [3]. In the PMM concepts, however, a homogeneous solid phase usually represents the heterogeneous fuel bed. Retrieving information on the level of individual solid particles needed for particle conversion submodels and the coupling between the submodels and the PMM can be challenging [4]. For example, when the particle heat transfer models require the particle diameter to calculate the surface area available for heat transfer or the individual particle temperature, a constant value or a distribution function often approximates the particle diameter, and average temperatures are assumed. There are similar limitations in the treatment of solid mass transport in the porous media model. Models based on the Discrete Element Method (DEM) allow on the other hand for the needed detail on the particle level but are due to the tracking of all particles computationally too heavy for large-scale applications and optimization purposes [5].

There have been many efforts to develop the PMM with the consideration of the heterogeneous features of the solid phase. Yang et al. [6] assumed the fuel bed to consist of three types of cells: void cells, solid surface cells, and solid inner cells. Intraparticle heat transfer was calculated in inner and surface cells. Johansson et al. [7] considered the intraparticle temperature gradients using a two-dimensional particle model. Heat transfer was modelled differently in the vertical and horizontal directions. Duffy et al. [8] designed a scheme for cell deformation due to shrinkage of the solid phase. The channelling effects in the fixed-bed were captured. Collazo et al. [9] developed a PPM in which the bed and freeboard were solved simultaneously, and the

---

[*] Corresponding author.
E-mail address: corinna.netzer@ntnu.no (C. Schulze-Netzer).

https://doi.org/10.1016/j.proci.2024.105575
Received 4 December 2023; Accepted 29 June 2024

geometry of the fuel particles of the cell was updated due to the temporal state. However, the movement of the solid phase during combustion is ignored by the above models, except for Duffy's model, which only considers vertical movement.

This study proposes an Eulerian bed model, including some of the features offered by DEM models and PMMs. Different shrinking core particle types representing the major thermal decomposition steps of solid fuels (wet matter, dry matter, char, and ash) are assigned to the computational grid. The solid mass in each grid cell is represented by fixed particle numbers with a homogeneous distribution of the four types of particles. The particle's properties are assigned to the grid cell and are updated when particles undergo thermal conversion and are transported between the cells. The particle's transportation is implemented by updating the registered number of each type of particle in both the involved grid cells. In this way, the properties of the solid phase are tracked by the unit of the computational cell, and the PMM can consider spatially dependent particle properties. When coupled with the gas phase model, solid phase properties are resolved statistically.

The approach is still based on an Eulerian model but features particle migration behaviour. In this study, only a simple bed collapse model that represents the bed shrinking has been implemented. However, in principle, the model's design could easily integrate particle movement models with arbitrary complexity. Each computational cell is the treated as a stochastic reactor for the solid particles. The migration model shall be interpreted such that a particle in one cell is exposed to a probability matrix determining the migration to any cell. With this, a cell is an elemental spatial region of all the particle's possible destinations. Generating the particle migration matrix between every two cells will be the key to implementing this particle migration model. It allows to efficiently and easily couple with other mesoscale models or even data-driven models to avoid the high computational costs attributed to the tracking of particle movements. Then, the model could easily extend its application to moving beds and even rotary kilns.

The paper first introduces the model framework and crucial submodels (Section 2) before validating the approach against an experiment from the literature and discussing the model performance in Section 3. The paper concludes with a summary of the model performance and suggestions for further improvements in future work.

2. Model description

This work aims to develop an Eulerian-based CFD model for simulations of the thermal conversion of packed beds. For the gas phase, the Navier–Stokes equations, including heat and mass transfer, will be resolved considering the phase fraction. For the solid phase, a grid cell-based particle conversion model has been developed and coupled with the new approach as a sub-grid model.

2.1. Model assumptions

The model is derived from certain physical and numerical assumptions. The main assumptions are:

1. The classification of solid particles is based on four particle types: wet wood, dry wood, char, and ash.
2. All particles of the same type within each computational cell are identical and are represented by a representative particle, hereafter called the representative particle.
3. All types of particles are modelled as spheres with a volume equivalent diameter and a Sauter mean diameter, which are stored and updated during the bed conversion process.
4. Representative particles can be converted to a different type in a conversion sequence, keeping the same particle number.
5. Particles can be transferred between two arbitrary cells while keeping the total number of particles unchanged. The cell that receives new particles will update its representative particle information according to averaging rules (described later).

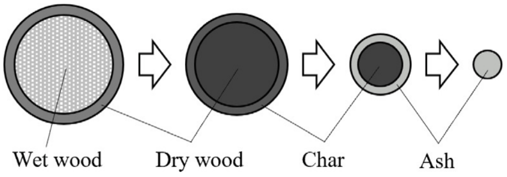

Fig. 1. Illustration of the sequential particle conversion models.

2.2. Biomass thermal conversation model

To present the particle-based Eulerian approach, concepts of the solid phase conversion model need to be known and are summarized briefly. A simplified layered particle model [10,11] is employed in this study following well-established principles. The model framework also allows for more advanced particle conversion models, which will be explored in future work. The current layered model implementation is, hence, an example demonstrating the ability of the overall modelling strategies. Fig. 1 shows the model concept. The four types of particles are labelled as wet, dry, char, and ash. These labels are used as subscripts in the following. All particles, except the ash particle, are described by the unreacted shrinking core approach, which has a core and a shell structure. The particle is assumed to have a homogeneous temperature and the conversions to occur on the front between the core and the shell. A fraction (θ) identifies the shell and core mass ratio. When the core is consumed completely, the particle type will change, and all particle information of the relevant type will be updated.

The particle temperature T_p is calculated based on the heat balance on the surface, which is given by:

$$m_{p,n}c_{p,n}\frac{dT_{p,n}}{dt} = q_{conv.,n} + q_{rad.,n} + S_{p,n}, \tag{1}$$

here, n is the particle type. It is worth noting that the particle's properties are the averaged properties rather than the intrinsic material properties. For example, the heat capacity of the wet wood particle, $c_{p,wet}$, is the average mass-weighted value between the wet wood core and the dry wood shell. $q_{conv.,n}$ is the heat convection term based on the particle's surface area, particle's temperature, gas phase temperature and the convective heat transfer coefficient and is calculated by Wakao's correlation [12] for the packed bed. $q_{rad.,n}$ is the heat exchange due to radiation, which will be further explained in Section 2.5. $S_{p,n}$ is the heat source term due to reaction or phase change. In this study, it also includes correction terms, which will be explained in Section 2.3.

During the thermal conversion process, the particle's mass (m_p) and fraction (θ) are updated according to the conversion rate (R) and solid yield (γ) following different processes. The particle mass changing and θ can be calculated as:

$$\frac{dm_{p,n}}{dt} = R_n(1-\gamma_n), \tag{2}$$

$$\frac{d(m_{p,n}\theta_n)}{dt} = R_n\gamma_n. \tag{3}$$

A simplified equilibrium model was implemented for the wet wood drying process. The drying rate is proportional to the difference between the equilibrium and current vapour concentrations in the gas phase [13]. In this study, wet wood and dry wood are treated as different materials; hence, the moisture mass loss rate is $R_{wet}M_w$, where M_w is the moisture content, and $\gamma_{wet} = 1 - M_w$.

The devolatilization model employed is a two-stage approach. The first step consists of three competing reactions. Products from dry wood conversion are gas, tar, and char [14]. The tar will partially convert into gas species and char in the second step. The char yield is determined by Arrhenius-type kinetics. The devolatilization is assumed to be a heat-neutral process. The implementation details are described in our previous study [10].

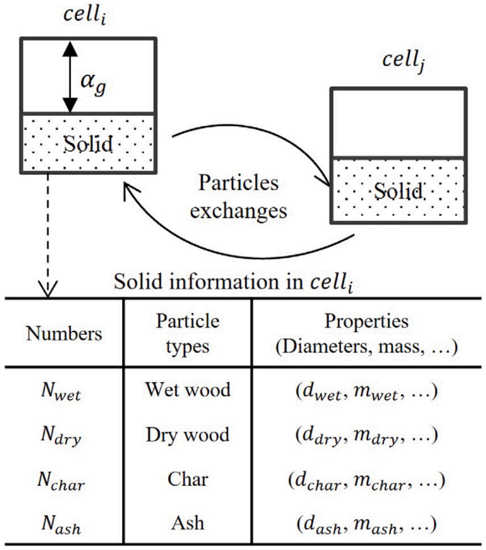

Numbers	Particle types	Properties (Diameters, mass, …)
N_{wet}	Wet wood	$(d_{wet}, m_{wet}, \ldots)$
N_{dry}	Dry wood	$(d_{dry}, m_{dry}, \ldots)$
N_{char}	Char	$(d_{char}, m_{char}, \ldots)$
N_{ash}	Ash	$(d_{ash}, m_{ash}, \ldots)$

Fig. 2. The concept of the solid bed model.

The charcoal burning model developed by Ström et al. [15] was adopted. The gas species diffusion through the ash shell is modelled using the effective mass diffusivity (D_{eff}):

$$D_{eff} = \varepsilon_{ash}^2 D_a. \tag{4}$$

The porosity of the ash layer will influence the diffusion rate of the reactants dominated by the temperature due to the melting of the ash. A sigmoid function approach was found by Ström et al. [15]. to mimic the melting effects:

$$\varepsilon_{ash} = \varepsilon_{lowT} - \frac{\left(\varepsilon_{lowT} - \varepsilon_{highT}\right)}{1 + \exp\left[-\frac{T - T_{Switch}}{\delta}\right]}. \tag{5}$$

There are two limiting properties ε_{lowT} and ε_{highT}, which are set as 0.9 and 0.01, respectively. The switch temperature T_{Switch} is set to 1473 K [15].

Shrinkage factors (η) are used to calculate the change of the particle's volume (V_p) [16]. The volume change rate is given by:

$$\frac{dV_{p,n}}{dt} = \eta_n \frac{R_n}{\rho_n}. \tag{6}$$

Since m_p and V_p are calculated based on the converting rate, in every particle time step, the equivalent spherical diameter (d_p), and the particle density (ρ_p) are updated. The Sauter mean diameter (d_{p32}) is calculated by assuming a constant particle sphericity.

When the shell-to-core fraction θ reaches 100%, the particle type changes. This type of change will not affect the particle's properties, such as mass, volume, temperature, etc.

2.3. Solid phase model

The solid phase consists of the four particle types described above and is modelled based on the CFD grid. For the solid phase region, each grid cell is assigned four representative particles and their particle numbers, constrained to be integers. As shown in Fig. 2, each cell will have a matrix that records the information of all the properties of the particle types. From the particles' properties, the solid phase's overall properties can be calculated. For example, the porosity of the bed, ε, can be calculated based on particle numbers and their volume. The solid phase properties are used in the coupling with the gas phase governing equation.

In addition to the coupling approach between the gas and the solid phase, there are two main purposes for the proposed bed model design. The first is to include particle motion phenomena. Because the particle numbers are integers, it is much more convenient to consider the exchange of particles between two grid cells. Details of the particle migration will be discussed in the next section. The other purpose is to calculate the heat transfer through the solid phase in an efficient way. The particles are only assigned to the grid cell without relative position information, hence the commonly used heat transfer models in the DEM framework is unfeasible. In this study, the PMM heat transfer model is adopted to correct the particle temperature due to conduction and radiation in the solid phase. During the simulation, the average solid phase temperature based on the particle temperature in the last time step is calculated using the particle's thermal mass (which is calculated as the product of the mass and the specific heat capacity) as the weight. Then, a temperature diffusion equation is resolved for the solid phase, which is given by:

$$(1-\varepsilon)\rho_s c_{p,s} \frac{\partial T_s}{\partial t} = k_{eff} \nabla \cdot T_s, \tag{7}$$

where, k_{eff} is the effective thermal conductivity of the solid phase. For the packing bed, it can be expressed as:

$$k_{eff} = k_e^g + k_e^c + k_e^r, \tag{8}$$

where, k_e^g is the effective conductivity through the fluid and point contact, k_e^c is the effective conductivity through the contact area, and k_e^r is the effective conductivity due to radiation. During the combustion process, the particle temperature is relatively high, and except in the later stage of the char burnout, the change of particle size is not significant. Therefore the most commonly used Zehner–Bauer–Schlünder (ZBS) [17] model is employed to predict $k_e^{g,c}$, and the Breitbach–Barthels (BB) [18] model is used to predict k_e^r. The Knudsen regime is neglected according to the Ref. [19]. The ZBS model is given by:

$$\frac{k_e^{g,c}}{k_f} = \left(1 - \sqrt{1-\varepsilon}\right) + \sqrt{1-\varepsilon}\left[\frac{\varphi}{\kappa} + (1-\varphi)k_c\right] \tag{9}$$

where, φ is a surface fraction parameter, and the value of 0.01 is used in this study [20]. k_c is calculated as:

$$\begin{aligned} k_c = {} & \left(\frac{2}{1-\kappa B}\right)\left[\frac{(1-\kappa)B}{(1-\kappa B)^2}\ln\left(\frac{1}{B\kappa}\right) \right. \\ & \left. - \frac{B+1}{2} - \frac{B-1}{1-\kappa B}\right], \end{aligned} \tag{10}$$

where, κ is the dimensionless conductivity ratio between the fluid and solid phase, which equals k_f/k_s. The deformation parameter B is related to the phase fraction, which is calculated as:

$$B = 1.25(1 - \varepsilon/\varepsilon)^{10/9}. \tag{11}$$

The general form for the thermal radiative conductivity for a unit cell in a packed pebble bed is defined as:

$$k_e^r = F_E 4\sigma d_p T_p^3, \tag{12}$$

where F_E is defined as the exchange factor. The benefit of using the exchange factor is that it is a dimensionless quantity and does not depend on the temperature. The BB model is given by:

$$\begin{aligned} F_E = {} & (1 - \sqrt{1-\varepsilon})\varepsilon \\ & + \frac{\sqrt{1-\varepsilon}}{2/\varepsilon - 1} \cdot \frac{B+1}{B} \cdot \frac{1}{1 + 1/[(2/\varepsilon - 1)\Lambda]}, \end{aligned} \tag{13}$$

where, Λ is dimensionless solid conductivity, which is defined as:

$$\Lambda = \frac{k_s}{4 d_p \sigma T_p^3}, \tag{14}$$

After resolving Eq. (7) for one time step, a new temperature field of the solid phase will be obtained. The difference between the old and new temperature fields gives the heat effect for the solid phase in each cell. The new temperature field will not be used to update the temperature of the solid phase directly. Instead, the heat effect is calculated as heat source/sink terms and redistributed to different types of particles based on thermal mass as part of the $S_{p,n}$ in Eq. (1). The solid phase temperature is updated by solving Eq. (1) and averaging calculation. Such corrections introduce numerical errors, especially when the temperature differences between different types of particles within one cell are significant. However, this is still an efficient way to consider solid phase radiation at high temperatures, and in such conditions, the convection calculation coupled with the gas phase will reduce the numerical inaccuracy.

2.4. Particle migration

As described above, the bed model allows the exchange of particles between different cells. Different mechanisms can cause particle motion; here bed collapsing because of particle shrinking during the conversion process is modelled. In this process, particles will gradually move along the direction of gravity due to volume changes. This study considers such movement using the collapse model by Duffy et al. [21]. In every time step, the solid volume fraction is updated. When the cell's porosity is larger than a given threshold of ε_{max}, different types of particles are chosen randomly from the above cell and transported downwards to pack its solid volume fraction back to the initial value ε_0. In this study, ε_{max} is given as 0.6, and ε_0 is 0.5, which is the initial random packing bed porosity. Since only an integer number of particles can be transported, there is a certain tolerance for ε_{max} and ε_0.

For each grid cell, every particle type is only allowed to have one representative particle. So, when a cell receives new particles, the particles must be merged with its representative particles in the same type. The merged new representative particles will take the average properties. Different particle properties will be calculated based on different averaging methods, but in general, the methods are linear calculations, except the d_p and d_{p32}, which use cubic mean and root mean square, respectively. Because the particles are already classified into four types, the linear merging mainly introduces inaccuracy to the reaction rates based on Arrhenius equations.

Beside particle migration, the thermal conversion degree can cause particle merging as well if in the current cell new particle type is already present. The same rules apply to this situation.

2.5. Sub-grid heat transfer

Eq. (7) resolves the heat conduction and radiation in the solid phase at the grid level and leaves the heat transfer between different types of particles within one cell uncovered. Especially when new particles are added to one cell by migration, this can cause immediate large temperature differences between different types of particles. As mentioned above, the convection heat transfer will smooth the difference, but the radiation at high temperatures remains significant to be considered.

The radiation control volume [22] approach is adopted to overcome this limitation. Since there is no information on the particle's relative position, it can be assumed that all the particles are evenly distributed. For each particle in the cell, a background average radiation temperature T_r can be defined as:

$$T_r^4 = \frac{\sum_n N_n A_{s,n} T_{p,n}^4}{\sum_n N_n A_{s,n}}, n = wet, dry, char, ash. \tag{15}$$

T_r is weighted by the particle number and surface area. Hence, the radiation term $q_{rad.,n}$ in Eq. (1) can be calculated as:

$$q_{rad.,n} = \epsilon\sigma A_{s,n}(T_{p,n}^4 - T_r^4), \tag{16}$$

where, ϵ and σ are the particle's emissivity and Stefan–Boltzmann constant, respectively. Eq. (16) and Eq. (7) are calculated at different scales. It is assumed that the view factor is uniform and the emissivities of different particle types are the same. Eq. (16) will not change the average solid phase temperature because, for one cell, the net heat flux is zero:

$$\sum_n \sum_{i=1}^{N_n} q_{rad.,n} = 0, n = wet, dry, char, ash. \tag{17}$$

2.6. Gas phase model

The gas phase governing equations with heat and mass transfer are listed in our previous work [10]. The momentum, heat, and mass transfers between the gas and solid phase are calculated through source terms. The standard $k-\epsilon$ turbulence model is used within Reynolds Averaged Navier–Stokes simulations (RANS). Lumped gas phase reactions considering the oxidization of H_2, CH_4, CO, and tar are computed by the eddy-dissipation-concept (EDC) model [10]. The radiation between the gas and solid phase is not considered because the widely-used modelling approach of resolving the radiative transport equation would cause the radiative heat in a high-temperature area to easily "penetrate" through the solid phase. This effect is known, especially when the CFD grid size is much larger than the particle size. Further, it would cause significant numerical errors on the front propagation process, which is the main modelling target of this study.

2.7. Solution algorithm

The simulations are performed using the following computational steps:

1. Based on the fluid grid, initialize solid phase properties.
2. Exchange particles between grid cells, update particle properties due to number changing and update the mean properties of the solid phase.
3. Calculate particle conversion submodels for all particle types.
4. Resolve the solid phase heat transfer Eq. (7), calculate the sub-grid particle radiation model and heat convection model, update particles' temperature.
5. Resolve the gas phase governing equations.
6. Advance one time step; if it is not finished, go back to Step 2.

3. Results and discussion

The new model is implemented using the open-source CFD toolbox OpenFOAM 7 [23]. The model is validated against the experimental data by Ström et al. [15]. As shown in Fig. 3, the experiments used a rectangular fixed-bed combustor, and was operated in a counter-current mode, which means that the combustion front moves downwards against the airflow. A two-dimensional (2D) simulation was carried out, and the computational domain has a geometry of $300\ \text{mm} \times 600\ \text{mm} \times 25\ \text{mm}$. Three meshes with different resolutions were tested: coarse ($12 \times 24 \times 1$), medium ($15 \times 30 \times 1$), and fine ($20 \times 40 \times 1$).

The combustor was operated with different air-flow rates. The walls of the combustor were considered as adiabatic. The material properties for the set-up of the fuel-bed are summarized in Table 1. According to Thunman's work [16], the shrinkage factors for the drying, devolatilization, and char burnout processes were chosen as 0.1, 0.39, and 0.95, respectively. The thermal properties used were the same as our previous work [10].

3.1. Grid size effects

Since the gas phase is resolved at a large average scale, the flow fields are rather uniform. This flow also dominates the downstream field after the combustion layer. The bed combustion rate using different air-flow rates were predicted with also different meshes. As shown in Fig. 4, for low air-flow rates, the model predictions agree well with the experiments for all grid sizes. When the air-flow rates are high, the bed model over-predicted the convection cooling effects, resulting in an

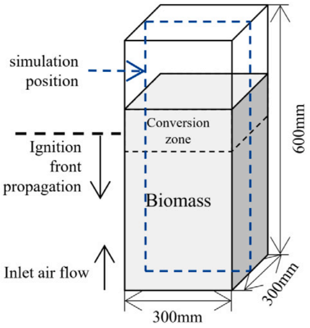

Fig. 3. Illustration of the biomass bed used in the experiment. 2D simulation carried out at 150 mm in the *z*-direction.

Table 1
Properties of biomass used in the simulation.

Description (units)	Value
Particle diameter (mm)	9.6
Particle intrinsic density, d.b. (kg/m^3)	1258
Moisture content, w.b. (%)	7
Ash content, d.b. (%)	0.25
Sphericity (–)	0.872
Bed packing porosity (–)	0.5

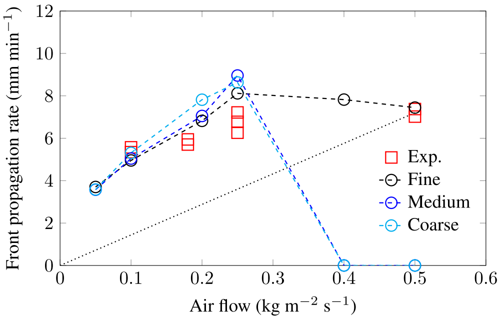

Fig. 4. The rate of the solid bed combustion at different air-flow rates. The red square indicates the results from the experiment [15]. The circle and dashed line show the calculated results using various grid sizes. The black dashed line indicates the stoichiometric limit.

early extinction for the cases with the coarser grid. Only the finest mesh is able to predict the correct burning rate at high air flow, yet this is an improvement of earlier model approaches, which are not able to predict burning for such high air flows. Likely, the absence of the radiation heat transfer between the gas and the solid phase could also cause early extinction but is neglected in the current model. As mentioned above, it is difficult to consider inter-phase radiation at the ignition front. The results from the fine mesh simulations seemed to show accurate predictions over the entire range of air flows; however, it was not in steady burning as it showed in the oxygen limited regime. Even with the high air-flow rates, the bed remained unburned, especially in the near wall region. Fig. 5 shows that the ignition propagation rates at the bed middle were much faster than at the near wall region. This is for the finest mesh and highest air flow.

Fig. 4 shows that the grid size does not significantly influence the combustion rate. However, the transient state of the bed during the conversion process largely depends on the grid size. In case of steady burning in the oxygen-limited regime (Fig. 6), the bed burned layer by layer (one layer of particles is defined as one layer of the grid cells at the same height), resulting in periodic oscillations of the bed temperature, mass loss rates due to conversion process, as well as the bed composition in the burning layer. Since the simulation is 2D, all mass is normalized with the raw bed mass per mm, the unit is hence mm min^{-1}. The oscillation periods are proportional to the grid size, which is also a consequence of uniform packing. Due to the representative particle approach, the particle type change in one cell due to conversion can only happen to all the particles within the same particle type in the same cell. Since the particle numbers in the cells are larger for medium and coarse meshes, the particle type change may get delayed in these cases. This could explain the early extinction of the bed for the coarse grid cases, since no char particle under the ignition front has been produced before the existing char burnout reached. The grid size is still not a pure numerical convergence problem, but is required by the submodels assumptions, which is a known problem in multi-phase modelling [24].

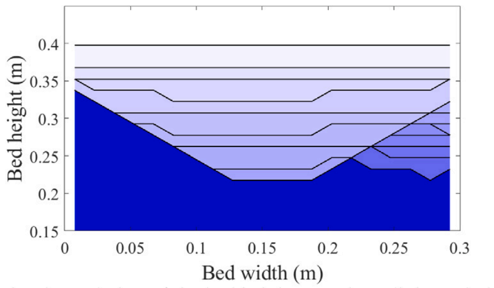

Fig. 5. Evolution of the bed height over time (light to dark), with fine mesh and an air-flow rate of 0.5 kg m^{-2} s^{-1}.

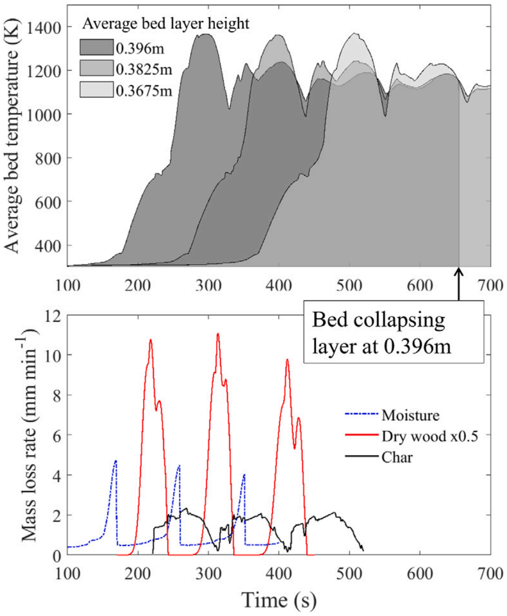

Fig. 6. Time evolution of the char layer front of the fuel bed, with fine mesh and an air-flow rate of 0.2 kg m^{-2} s^{-1}.

3.2. Radiation heat transfer and particle migration effects

Previous research showed that heat transfers through particle-to-particle radiation and particle-to-gas convection are crucial for maintaining the ignition front propagating [24]. In this section, the implemented submodels are briefly evaluated. For comparative reasons, selected case simulations were conducted without adopting the collapse model described in Section 2.4 and the sub-grid radiation model described in Section 2.5, individually. In addition, an alternative approach yielding a higher exchange factor F_E in Eq. (12) proposed by Johnson et al. [25] has been adopted for comparison.

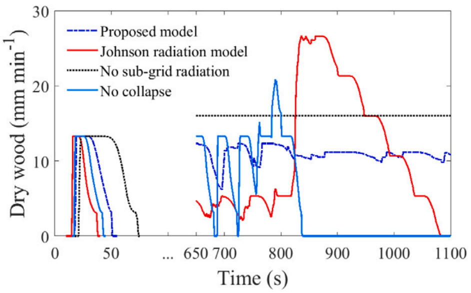

Fig. 7. Dry wood evolution over time for different activated submodels, with fine mesh and an air-flow rate of 0.2 kg m^{-2} s^{-1}. (The left part of the figure is at the starting phase in the top layer. The particle undergoes first drying, producing dry wood mass and thermal conversion, reducing the dry wood mass. At the right part of the figure at the end of the simulation, the divergence between the models is shown.)

The evolution of dry wood mass is used to evaluate the effect of the submodels on bed conversion and is shown in Fig. 7. This is the most sensitive property because the dry wood is mainly produced and consumed near the ignition front in the simulations. At the early stage, the simulation without the sub-grid radiation included predicts a much slower conversion rate. Johnson's model predicts a faster heat transfer rate than the BB model. The simulation using the Johnson's model shows, however, certain unsteady burning during the conversion. The simulation without the collapse model shows a faster conversion process. This is mainly due to that the char burnout process is enhanced with a larger bed voidage and more heat being released from the top. The simulated ignition front, either with the Johnson's model or without the collapse model, reaches the bottom of the bed with a significantly over-predicted propagation rate. In the simulation without collapse model, some unburned char particles are suspended in the bottom part of the bed.

4. Conclusions

A novel model for solid fuel combustion has been developed and validated against experiments of a fixed-bed combustor. The results show that the model agrees well with the experiment in the oxygen-limited combustion regime. This is a significant improvement compared to similar simplified bed models as the current model features physical processes such as migration behaviour and inter-particle radiation. However, due to the simplified treatment of the particle's geometry information, the model tends to over-predict the convective cooling effects at higher inlet air flow rates, resulting in a too early extinction.

The model also focused on heat transfer modelling in the solid phase. The conventional thermal diffusion model with effective solid phase conductivity is considered; meanwhile, the sub-grid level radiation between the solid phase is calculated. During high-temperature combustion, the accurate calculation of the solid radiation is crucial to predict the solid phase temperature profile and the ignition propagation process. This advanced heat transfer treatment is crucial to replicate the experiment.

Using the finest mesh in the analysis, the experiment is well predicted, even in challenging high airflow conditions. The main reason for this good agreement with the experiment is the associated inhomogeneous bed layer burnout. In the coarse mesh setups, the local flame propagation is extinct due to the delay in changing the particle type. Further validation is needed to investigate the mesh dependency.

In general, the model proposes a new efficient framework for the large-scale solid fuel combustion process and is capable of keeping a distinctive heterogeneity of the solid phase. There remains room for improvements of the submodels in terms of more physical particle conversion models, particle migration models, particle properties distribution models, etc. It has, however, great potential for a wide range of applications related to solid fuel conversion processes.

Novelty and significance statement

The novelty of this research is to establish a new Eulerian-Eulerian porous media formulation capable of simulating the conversion of a solid fuel bed and its motion. The proposed approach combines the advantages of the higher computational efficiency from Eulerian-Eulerian porous media models and includes fundamental physical processes, such as particle shrinkage and bed motions, typically modelled in the Eulerian-Lagrangian framework. This is done by registering particle properties via scalar fields on the Eulerian grid. The new model allows us to improve state-of-the-art heat transfer modelling in the bed by including particle-particle radiation and convection. Treating the solid as a particle ensemble allows the transfer of particles to lower bed layers - a mechanism needed for bed collapsing. This novel low computational cost treatment will enable us in the future to simulate large grate-fired furnaces with reasonable computational cost and a high degree of accuracy.

CRediT authorship contribution statement

Jingyuan Zhang: Designed the model concept and research, Performed the simulations and analysis, Wrote the manuscript. **Corinna Schulze-Netzer:** Model conceptualization and research, Performed post-processing, Revised the manuscript. **Tian Li:** Model conceptualization and research, Revised the manuscript. **Terese Løvås:** Conceptualization and research, Revised the manuscript.

Declaration of competing interest

The authors declare that they have no known competing financial interests or personal relationships that could have appeared to influence the work reported in this paper.

Acknowledgements

The authors acknowledge support from the Research Council of Norway and a number of industrial partners through the BioCarbUp project (294679) and BioSynGas project (319723).

References

[1] N. Klinghoffer, N. Themelis, M. Castaldi, Waste to energy (WTE): an introduction, in: Waste to Energy Conversion Technology, Elsevier, 2013, pp. 3–14.
[2] T. Christensen, Solid Waste Technology and Management, John Wiley & Sons, 2011.
[3] M.R. Karim, J. Naser, CFD modelling of combustion and associated emission of wet woody biomass in a 4 MW moving grate boiler, Fuel 222 (2018) 656–674.
[4] H. Ström, H. Thunman, CFD simulations of biofuel bed conversion: A submodel for the drying and devolatilization of thermally thick wood particles, Combust. Flame 160 (2) (2013) 417–431.
[5] A.H. Mahmoudi, X. Besseron, F. Hoffmann, M. Markovic, B. Peters, Modeling of the biomass combustion on a forward acting grate using XDEM, Chem. Eng. Sci. 142 (2016) 32–41.
[6] Y.B. Yang, C. Ryu, A. Khor, V.N. Sharifi, J. Swithenbank, Fuel size effect on pinewood combustion in a packed bed, Fuel 84 (16) (2005) 2026–2038.
[7] R. Johansson, H. Thunman, B. Leckner, Influence of intraparticle gradients in modeling of fixed bed combustion, Combust. Flame 149 (1–2) (2007) 49–62.
[8] N. Duffy, Investigation of Biomass Combustion in Grate Furnaces Using CFD (Ph.D. thesis), 2012.
[9] J. Collazo, J. Porteiro, D. Patiño, E. Granada, Numerical modeling of the combustion of densified wood under fixed-bed conditions, Fuel 93 (2012) 149–159.
[10] J. Zhang, T. Li, H. Ström, T. Løvås, Grid-independent Eulerian-Lagrangian approaches for simulations of solid fuel particle combustion, Chem. Eng. J. 387 (2020) 123964.
[11] T. Li, H. Thunman, H. Ström, A fast-solving particle model for thermochemical conversion of biomass, Combust. Flame 213 (2020) 117–131.
[12] N. Wakao, S. Kagei, Heat and Mass Transfer in Packed Beds, vol. 1, Taylor & Francis, 1982.
[13] S. Tavakkol, T. Zirwes, J.A. Denev, F. Jamshidi, N. Weber, H. Bockhorn, D. Trimis, An Eulerian-Lagrangian method for wet biomass carbonization in rotary kiln reactors, Renew. Sustain. Energy Rev. 139 (2021) 110582.

[14] H. Lu, G. Peirce, B. Ripa, L.L. Baxter, Comprehensive study of biomass particle combustion, Energy Fuels 22 (4) (2008) 2826–2839.
[15] H. Ström, F. Niklasson, A. Hjörnhede, S. Hermansson, Experimental and numerical investigations of ash behaviour in fixed-bed combustion of woody biomass pellets, Journal of the International Flame Research Foundation (ISSN: 2075-3071) (2018) 201612.
[16] H. Thunman, B. Leckner, F. Niklasson, F. Johnsson, Combustion of wood particles—a particle model for Eulerian calculations, Combust. Flame 129 (1–2) (2002) 30–46.
[17] R. Bauer, E. Schlunder, Effective radial thermal conductivity of packings in gas flow. Part I. Convective transport coefficient, Int. Chem. Eng. 18 (2) (1978) 189–204.
[18] G. Breitbach, H. Barthels, The radiant heat transfer in the high temperature reactor core after failure of the afterheat removal systems, Nucl. Technol. 49 (3) (1980) 392–399.
[19] Y. Qian, Z. Han, J.-H. Zhan, X. Liu, G. Xu, Comparative evaluation of heat conduction and radiation models for CFD simulation of heat transfer in packed beds, Int. J. Heat Mass Transfer 127 (2018) 573–584.
[20] W. Van Antwerpen, C. Du Toit, P.G. Rousseau, A review of correlations to model the packing structure and effective thermal conductivity in packed beds of mono-sized spherical particles, Nuclear Eng. Des. 240 (7) (2010) 1803–1818.
[21] N.T. Duffy, J.A. Eaton, Investigation of factors affecting channelling in fixed-bed solid fuel combustion using CFD, Combust Flame 160 (10) (2013) 2204–2220.
[22] R. Mehrabian, A. Shiehnejadhesar, R. Scharler, I. Obernberger, Multi-physics modelling of packed bed biomass combustion, Fuel 122 (2014) 164–178.
[23] OpenFOAM 7, 2019, http://openfoam.org/.
[24] J. Zhang, T. Li, H. Ström, T. Løvås, Computationally efficient coarse-graining XDEM/CFD modeling of fixed-bed combustion of biomass, Combust. Flame 238 (2022) 111876.
[25] E. Johnson, İ. Tarı, D. Baker, A Monte Carlo method to solve for radiative effective thermal conductivity for particle beds of various solid fractions and emissivities, J. Quant. Spectrosc. Radiat. Transfer 250 (2020) 107014.